IEEE Access
Multidisciplinary | Rapid Review | Open Access Journal

Received 31 August 2023, accepted 20 September 2023, date of publication 25 September 2023,
date of current version 28 September 2023.

Digital Object Identifier 10.1109/ACCESS.2023.3318737

RESEARCH ARTICLE

Day-Ahead and Intra-Day Economic Dispatch of Electricity Hydrogen Integrated Energy System With Virtual Energy Storage

XINGHUA LIU[1], (Senior Member, IEEE), LONGYU ZU[1], (Student Member, IEEE), XIANG LI[1], (Student Member, IEEE), HUIBAO WU[2], RONG HA[3], AND PENG WANG[4], (Fellow, IEEE)

[1]School of Electrical Engineering, Xi'an University of Technology, Xi'an 710048, China
[2]State Grid Xi'an Electric Power Supply Company, Xi'an 710000, China
[3]Xi'an Jinze Electric Technology Company Ltd., Xi'an 710100, China
[4]School of Electrical and Electronic Engineering, Nanyang Technological University, Singapore 639798

Corresponding author: Xinghua Liu (liuxh@xaut.edu.cn)

This work was supported in part by the National Natural Science Foundation of China under Grant U2003110, and in part by the High-Level Talents Plan of Shaanxi Province for Young Professionals.

ABSTRACT In this paper, a model of electricity hydrogen integrated energy system considering virtual energy storage is proposed to enhance the penetration rate of renewable energy. Specifically, mathematical modeling is conducted for the integrated energy system of electricity hydrogen. Considering the thermal characteristics of buildings and demand response from users, the virtual energy storage system is integrated into the model to optimize the system's overall performance. A day-ahead and intra-day optimization scheduling strategy is proposed to address the uncertainties of renewable energy generation, load forecasting, and power fluctuations. The day-ahead optimization model coordinates the output of various components to minimize the daily operating costs, resulting in a 24-hour operational plan. The intra-day scheduling model aims to smooth out power fluctuations and improve system stability by refining the day-ahead strategy through rolling optimization. Four comparative cases are presented to validate the proposed model. The quantitative results of this study show that introducing a virtual energy storage system has multiple significant advantages in an electric hydrogen integrated energy system. By optimizing operational costs, the equipment cost of the system is significantly reduced, and the integration of renewable energy is dramatically improved, effectively promoting sustainable development. In addition, the application of virtual energy storage maximizes the advantages of hydrogen energy while helping to reduce carbon emissions, providing strong support for the future sustainability of the energy system.

INDEX TERMS Electricity hydrogen integrated energy systems, virtual energy storage, demand response.

NOMENCLATURE

P^t_{ebuy}	Electricity purchased from the power grid.
P^t_{gbuy}	Power of gas purchased from the gas network.
P^t_{GT}	Power generation of gas turbines.
P^t_{PV}	Photovoltaic output.
P^t_{WT}	Wind power output.
P^t_{HFC}	Power generation of hydrogen fuel cells.
P^t_{eload}	Electric load per hour at the user end.
P^t_{hload}	Thermal load on the load side.
P^t_{cload}	Cold load on the load side.
P^t_{ELe}	Electricity consumption of electrolysis device.
P^t_{EB}	Hourly electricity consumption of electric boilers.
P^t_{AC}	Power consumption of the electric air conditioner.

The associate editor coordinating the review of this manuscript and approving it for publication was Jorge Esteban Rodas Benítez.

P^t_{GTg}	Natural gas consumed by the gas turbine.
P^t_{HFCh}	Hydrogen power consumed by the fuel cell.
P^t_{ELh}	Hydrogen production power of the electrolysis device.
P^t_{MRh}	Hydrogen consumption of the methanation unit.
P^t_{MRg}	Natural gas produced by the methanation unit.
Q^t_{EB}	Heat output of the electric boiler.
Q^t_{AC}	Cooling power of the electric air conditioner.
Q^t_{HS-dis}	Heat dissipation capacity of the heat storage tank.
Q^t_{HS-cha}	Charging power of heat storage tank.
Q^t_{ARin}	Thermal power consumed by the absorption chiller.
Q^t_{GBg}	Natural gas power consumed by the gas boiler.
Q^t_{HFC}	Heat generation of hydrogen fuel cells.
Q^t_{AR}	Cooling capacity of the absorption chiller.
Q^t_{GB}	Heat generated by gas boilers.
Q^t_{WH}	Heat generated by waste heat boiler.
Q^t_{GT}	Heat generated by gas turbines.
η^e_{GT}	Power generation efficiency of a gas turbine.
η^e_{HFC}	Power generation efficiency of hydrogen fuel cells.
η_{EL}	Electrolysis efficiency of the electrolysis device.
η_{EB}	Heat production efficiency of the electric boiler.
η_{AC}	Cooling efficiency of the electric air conditioner.
η_{MR}	Gas production efficiency of the methanation unit.
η_{GB}	Heat production efficiency of the gas boiler.
η_{WH}	Heat production efficiency of the waste heat boiler.
η^h_{HFC}	Heat release efficiency of the hydrogen fuel cell.
η_{EB}	Heat release efficiency of the electric boiler.
η^h_{GT}	Heat production efficiency of the gas turbine.
η_{AR}	Cooling efficiency of the absorption refrigerator.
σ_{HS}	Self-loss rate of the heat storage tank.
η^{cha}_{HS}	Charging efficiency of the heat storage tank.
η^{dis}_{HS}	Heat release efficiency of the heat storage tank.
S^t_{HS}	Capacity of heat storage tank at time t.
S^0_{HS}	Capacity of the initial state of the heat storage tank.
ρ	Air density.
V	Air specific heat capacity.
T_{in}	Indoor temperature.
T^t_{out}	Outdoor temperature.
$k_{wall}k_{win}$	Heat transfer coefficient of the external wall of the building.
F_{wall}	Area of the external wall of the building.
F_{win}	Heat transfer area of the external wall of the building.
I	Solar radiation power.
SC	Sun shading coefficient.
$P^{\min}_{GT}P^{\max}_{GT}$	Upper and lower limits of gas turbine electromechanical power.
$Q^{\min}_{GT}Q^{\max}_{GT}$	Upper and lower limits of thermal power for gas turbine.
$Q^{\min}_{GB}Q^{\max}_{GB}$	Upper and lower limits of thermal power for gas boilers.
$Q^{\min}_{EB}Q^{\max}_{EB}$	Upper and lower limits of gas electric heating power.
$Q^{\min}_{WH}Q^{\max}_{WH}$	Upper and lower limits of the electric heating power of the waste heat boiler.
$Q^{\min}_{AR}Q^{\max}_{AR}$	Upper and lower limits of the cooling power of the absorption refrigeration mechanism.
$Q^{\min}_{AC}Q^{\max}_{AC}$	Upper and lower limits of the cooling power of the electric air conditioner.
$P^{\min}_{EL}P^{\max}_{EL}$	Upper and lower limits of the operating power of the electrolytic cell.
$P^{\min}_{MR}P^{\max}_{MR}$	Upper and lower limits of the operating power of the methanation device.
$P^{\min}_{HFC}P^{\max}_{HFC}$	Upper and lower limits of fuel cell operating power.
$Q^{\min}_{HS-dis}Q^{\max}_{HS-dis}$	Upper and lower limits of the heat release power of the heat storage tank.
$\Delta P^{\min}_{GT}\Delta P^{\max}_{GT}$	Upper and lower limits of gas turbine climbing rate.
$\Delta P^{\min}_{ELe}\Delta P^{\max}_{ELe}$	Upper and lower limits of the climbing rate of the electrolytic cell.
$\Delta P^{\min}_{MRh}\Delta P^{\max}_{MRh}$	Upper and lower limits of methane reactor climbing rate.
$\Delta P^{\min}_{HFCh}\Delta P^{\max}_{HFCh}$	Upper and lower limits of fuel cell climbing rate.
$S^{\min}_{HS}S^{\max}_{HS}$	Upper and lower limits of the capacity of the heat storage tank.

I. INTRODUCTION

The gradual depletion of fossil fuels, increased environmental pollution, and increased carbon dioxide emissions have posed a significant challenge to the global energy mix. Energy production and consumption patterns must be adjusted to

meet social development needs. The integrated energy system (IES) integrates cooling, heating, electricity, and gas and promotes renewable energy development. Therefore, integrated energy systems have become an advanced topic in energy research [1]. Low-carbon goals can be achieved by transitioning wind, photovoltaic, and other new energy sources from alternative to dominant power sources because they are low-cost and carbon-emission-free [2]. The grid integration of renewable energy sources is a common challenge for integrated energy systems as the generation of renewable energy is influenced by natural factors such as insolation and wind speed. The power of renewable energy sources fluctuates with weather and time of day, and the output of wind and photovoltaic (PV) power generation is volatile and uncertain, increasing the pressure on the system and peaking in large-scale grid integration [3], [4]. For the grid to ensure flexible resources to stabilize power supply and demand, how to promote new energy consumption is a critical issue that needs to be solved nowadays [5].

The instability and volatility of renewable energy sources (e.g., wind, solar) may impact the power system, generating power surpluses and power shortages at other times. By coordinating natural gas generators, power-to-gas (P2G) technology, and natural gas storage technology, it is expected to alleviate energy shortages and accommodate renewable energy sources in an integrated electric-gas system (IEGS) [6]. Hydrogen is considered a promising energy carrier with an essential role in areas where direct electrification is challenging to achieve, especially in achieving deep decarbonization, where renewable energy is directly converted to hydrogen energy and where hydrogen is prepared through water electrolysis, which converts unstable electrical energy into a storage-stable hydrogen fuel, which can be used for heating, fuel cell power generation, and other applications. Hydrogen production through water electrolysis in a P2G plant and carbon dioxide from conventional power generation exhaust is a promising method of producing synthetic natural gas [7]. Although hydrogen is complex to store and transport on a large scale, it has a high energy conversion efficiency. In contrast, synthetic natural gas can be stored and transported on a large scale through natural gas pipeline systems, but it has a low energy conversion efficiency. Therefore, an electric-hydrogen-integrated energy system (EH-IES) was established by combining the advantages of high hydrogen conversion efficiency and large-scale natural gas storage [8]. EH-IES has been studied to some extent. Literature [9] provided an integrated modeling framework for electricity, hydrogen, and methane systems and developed a market equilibrium model for the integrated system model of electricity and natural gas. Literature [10] proposed a day-ahead economic optimization dispatch model for regional electric-hydrogen integrated energy systems (REHIES) with high renewable energy penetration. The electricity-hydrogen coupling device in the model is represented using an energy storage device and an insensitive electrical load (ISEL), thus optimizing the economic efficiency of the integrated electricity-hydrogen energy system. In the future, using renewable energy sources to prepare hydrogen, the electric-hydrogen integrated energy system can help reduce the use of fossil fuels, lower greenhouse gas emissions, promote a low-carbon and carbon-neutral energy transition, and provide new outlets for hydrogen applications, such as hydrogen fuel cell vehicles and industrial hydrogen, which is expected to encourage the development of hydrogen energy technology.

The operation and scheduling of existing integrated energy systems are mainly based on fixed load demands, and the output of each device is optimized primarily to the regulation capability of energy storage devices [11]. The high construction and operation costs of energy storage devices pose a significant challenge for large-scale implementation. To solve this problem, the concept of virtual energy storage (VES) has been proposed. Virtual energy storage utilizes alternative devices and scheduling strategies to achieve energy balance within the system, thereby improving system operation's reliability and economic efficiency. By shifting or converting the energy output of various energy devices, VES provides a viable alternative to deploying expensive physical energy storage technologies. Literature [12] developed a multi-objective optimization model for virtual energy storage in building microgrids based on the thermal storage characteristics of the building itself. Flexible and controllable loads, especially heating, ventilation, and air [13] conditioning (HVAC) systems, can provide similar energy storage services to the system by modifying their requirements. Literature [14] is mainly based on demand-side controllable load management and peak and valley tariff systems. ''Peak shaving'' is a load management strategy that utilizes energy peak management techniques to increase electricity consumption during off-peak hours and decrease electricity consumption during peak hours. This approach helps to manage the load on the grid by reducing the peak electricity use and shifting it to off-peak hours. Literature [15] aims to tap into the potential of demand response by flexibly guiding users' energy consumption and EV behavior (charging, discharging, and providing spinning reserve) to promote the balance between energy supply and demand.

Meanwhile, many studies have proposed multi-timescale optimization models to reduce the adverse effects of power fluctuations on the system. Multi-timescale-based optimal dispatch strategies aim to develop optimal decisions to maximize system performance by integrating system demands and constraints at different timescales. The impact of renewable energy and load uncertainty on the dispatch results can be reduced by exploiting the fact that the prediction accuracy gradually improves with decreasing time scales. To obtain the optimal economic dispatch of an Electric-Hydrogen Integrated Energy System (E-HIES), Zhang et al. [16] proposed an optimal dispatch model based on day-ahead long-term optimization and intra-day Model Predictive Control (MPC)

hierarchical rolling optimization. Cheng et al. [17] proposed an Energy Hub (EH) with multi-energy streams and multiple types of energy storage systems (MESS), a Multi-Scale Coordinated Optimization (MTSCO) approach that integrates the effects of variable energy resources (VERs) and load demand uncertainty on scheduling plans. Li et al. [18] proposed a hybrid timescale energy optimization scheduling model based on the supply and demand game in response to the complex energy coupling and the competition of multi-market players in an integrated energy system.

Based on the above studies, we propose an electric-hydrogen integrated energy system with virtual storage [19]. The electric hydrogen production technology in the electric-hydrogen integrated energy system can consume abandoned wind and light and optimize wind and light scheduling. When the wind and fair supply are sufficient, the energy that exceeds the electricity demand can be used to electrolyze water to prepare hydrogen, and the electricity generated from renewable energy sources can be converted into hydrogen and stored for emergency use. The building virtual energy storage system can absorb and store thermal energy when there is sufficient light, coupling it with the supply of renewable energy, and the excess of renewable energy can be used to heat the building, increasing the efficiency of integrated energy utilization and providing a comfortable temperature range for users. On the other hand, the demand response virtual energy storage system allows for flexible management of controllable loads, adjusting energy consumption patterns according to the volatility and intermittency of energy supply. In times of tight power supply, energy demand can be reduced by adjusting the hours of use of equipment and reducing the use of energy-consuming equipment, thereby balancing energy supply and demand. A day-ahead economic dispatch model has been developed to improve the economic efficiency of the Integrated Energy System (IES), incorporating day-ahead and intra-day rolling optimization. The model considers the impact of renewable energy sources and load variations on the operational flexibility of the IES. The day-ahead operating schedule provides a margin for system flexibility. Meanwhile, the intraday rolling optimization adjusts the output of each device to accommodate long-term power fluctuations and stabilizes the rapid changes in electrical energy in the short term. The main contributions of this study can be summarized as follows:

1) Incorporate building virtual energy storage into the optimal scheduling model of EH-IES. This inclusion not only meets users' comfort requirements but also effectively reduces the system's operating costs while maintaining user comfort.
2) Consider user-side demand response as virtual energy storage participating in system economic dispatch can reduce storage costs and enhance system-user connectivity.
3) A multi-time-scale dispatch strategy considering renewable energy and load fluctuations from day-ahead to intra-day can stabilize power oscillations in short-term and long-term operations.

The structure of this paper is organized as follows. In Section II, the EH-IES framework is proposed, and a mathematical model for EH-IES is established. Section II presents the concept of virtual energy storage and sets the mathematical models for building virtual energy storage and user-side demand response virtual energy storage. Section IV describes a multi-time scale economic optimization scheduling strategy, including day-ahead and intra-day. In Section V, the effectiveness of the proposed method is demonstrated through results from four case studies. Finally, the conclusion is presented in Section VI.

II. EH-IES STRUCTURE AND EQUIPMENT MODEL

A. EH-IES STRUCTURE

The structure of the EH-IES is shown in Fig. 1. The EH-IES uses energy production, conversion, and storage equipment to meet the demand for electricity, heating, cooling, and hydrogen, in addition to purchasing electricity and natural gas from the grid and the gas network to make up for energy shortfalls [20]. Due to the uncertainty of renewable energy sources such as electrolysis, units consume wind and solar, redundant wind PV, and some of the hydrogen produced is mixed with natural gas for gas turbines. A portion of the hydrogen is used by hydrogen fuel cells to create electric power for the user side, electric chillers, and electric boilers [21]. The electric power generated by the gas turbine consuming natural gas can be directly supplied to the user. At the same time, the waste heat generated by the gas turbine is absorbed by the waste heat boiler, which is provided directly to the user side. The absorption chiller absorbs part of this to generate cooling power. Electric boilers and gas boilers are the leading heat power supply equipment; electric boilers need to consume electricity to produce heat, gas boilers need to consume natural gas to have heat power, and the excess heat produced by the system is stored in the heat storage tank. Cold power is mainly supplied to users by electric chillers and absorption chillers.

B. MODELING OF ENERGY CONVERSION AND STORAGE EQUIPMENT

The electric balance equation is presented as follows, which considers the energy input and output of the power sector, including photovoltaic, WT, GT, HFC, energy transmitted by the grid, power load, AC, and EB.

$$P^{t}_{\text{ebuy}} + P^{t}_{GT} + P^{t}_{PV} + P^{t}_{WT} + P^{t}_{HFC} = P^{t}_{eload} + P^{t}_{ELe} + P^{t}_{EB} + P^{t}_{AC} \tag{1}$$

$$\begin{cases} P^{t}_{GT} = \eta^{e}_{GT} P^{t}_{GTg} \\ P^{t}_{HFC} = \eta^{e}_{HFC} P^{t}_{HFCh} \\ P^{t}_{ELe} = P^{t}_{ELh}/\eta_{EL} \\ P^{t}_{EB} = Q^{t}_{EB}/\eta_{EB} \\ P^{t}_{AC} = Q^{t}_{AC}/\eta_{AC} \end{cases} \tag{2}$$

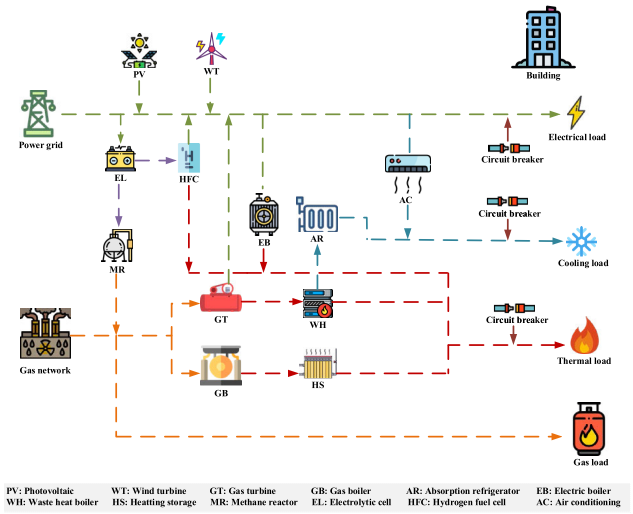

FIGURE 1. Structure of EH-IES.

The gas supply of the gas hub is provided by the gas and MG transmitted through the gas network. The energy output includes gas load, GT, and GB. The gas balance equation is expressed as follows:

$$\begin{cases} P^t_{ELh} = P^t_{MRh} + P^t_{HFCh} \\ P^t_{gbuy} + P^t_{MRg} = P^t_{GTg} + Q^t_{GBg} \end{cases} \tag{3}$$

$$P^t_{MRg} = \eta_{MR} P^t_{MRh} \tag{4}$$

The energy input of the heating hub consists of GT, GB, WH, and HFC, while the energy output consists of heat load, AC, and AR. The heat balance equation is presented as follows:

$$\begin{aligned} &Q^t_{HS-dis} + Q^t_{GB} + Q^t_{WH} + Q^t_{HFC} + Q^t_{EB} + Q^t_{GT} \\ &\quad = P^t_{hload} + Q^t_{HS-cha} + Q^t_{ARin} \end{aligned} \tag{5}$$

$$\begin{cases} Q^t_{GB} = \eta_{GB} Q^t_{GBg} \\ Q^t_{WH} = \eta_{WH} Q^t_{GT} \\ Q^t_{HFC} = \eta^h_{HFC} Q^t_{HFC} \\ Q^t_{EB} = \eta_{EB} P^t_{EB} \\ Q^t_{GT} = \eta^h_{GT} P^t_{GT} \\ Q^t_{ARin} = Q^t_{AR} / \eta_{AR} \end{cases} \tag{6}$$

The energy input of the cooling hub includes AR and AC, and the energy output is the cooling load. The cooling balance equation is as follows:

$$Q^t_{AC} + Q^t_{AR} = P^t_{cload} \tag{7}$$

$$\begin{cases} Q^t_{AR} = \eta_{AR} Q^t_{ARin} \\ Q^t_{AC} = \eta_{AC} P^t_{AC} \end{cases} \tag{8}$$

Heat storage equipment can charge and release heat through planned energy, and its general model is as follows:

$$\begin{cases} S^t_{HS} = S^{t-1}_{HS} (1 - \sigma_{HS}) + \left(\eta^{cha}_{HS} Q^t_{HS-cha} - \dfrac{Q^t_{HS-dis}}{\eta^{dis}_{HS}} \right) \Delta t \\ S^T_{HS} = S^0_{HS} \end{cases} \tag{9}$$

III. VIRTUAL ENERGY STORAGE SYSTEM

As the field of energy storage for IES continues to make significant progress, there is an increasing focus on leveraging flexible resources such as network-side dynamic characteristics and demand-side response to effectively balance power within the integrated energy system across various time intervals. This objective can be accomplished by implementing pipeline storage, spatiotemporal transfer of electricity, and utilizing physical energy storage devices like batteries and heat storage tanks [22]. Although virtual energy storage does not necessitate the construction of physical energy storage equipment, it can still have a comparable impact on the planning and operation of integrated energy systems [23]. Hence, this study explicitly investigates forms of virtual energy storage: the thermal storage characteristics of buildings and the demand-side response of the load side, which are included in the operational planning of the integrated energy system.

A. BUILDING HEAT STORAGE CHARACTERISTICS

Due to the enclosed structure of certain buildings, they possess a thermal mass property that contributes to the deceleration of indoor heat dissipation. The exploitation of these heat storage characteristics of the building proves advantageous in achieving optimal operation of the integrated energy system, as illustrated in Fig. 2. By considering the user comfort range, it becomes feasible to flexibly regulate the output of heating or refrigeration equipment, facilitating energy transfer over specific time intervals. This control strategy effectively transforms the building into a ''virtual energy storage'' component.

According to the law of energy conservation, the mathematical model of building virtual energy storage is obtained, as shown in (10):

$$\Delta Q = \rho C V \frac{dT_{in}}{d\tau} \tag{10}$$

Equation (10) can be reformulated as a difference equation taking into account the main factors that affect the internal heat of a building, such as the cold/heat dissipation caused by indoor and outdoor temperature differences, solar thermal radiation, heating of human bodies and equipment inside the building, and the cooling/thermal power output of refrigeration/thermal equipment. The resulting equation is shown follows:

$$\begin{aligned} \rho C V \frac{dT_{in}}{d\tau} &= k_{wall} F_{wall} \left(T^t_{out} - T^t_{in} \right) + k_{win} F_{win} \left(T^t_{out} - T^t_{in} \right) \\ &\quad + I F_{win} SC + Q^t_{in} - Q^t_{cl} \end{aligned} \tag{11}$$

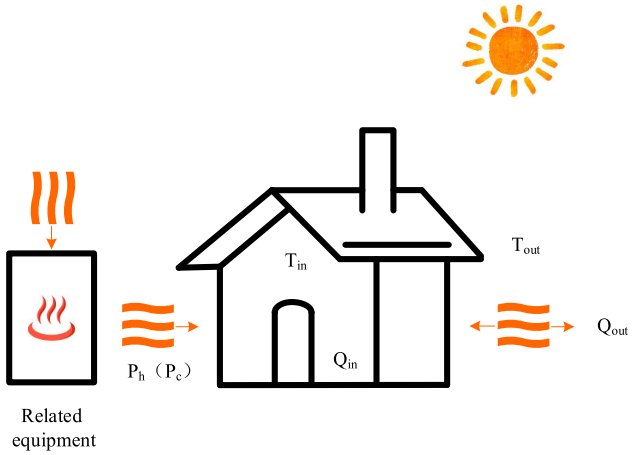

FIGURE 2. Building virtual energy storage structure.

B. DEMAND RESPONSE

Demand side response is a practical regulatory approach that offers flexibility and schedulability for shifting energy consumption patterns over time. By adjusting the load curve, demand-side response contributes to enhanced utilization of renewable energy sources. This paper establishes a demand-side response virtual energy storage model, incorporating price and incentive-based demand response mechanisms [24].

Price-based demand response (PDR) entails users adjusting their load demand during different periods based on variations in electricity prices throughout actual power consumption. This practice enables users to shift their energy consumption from peak hours to periods of lower demand [25]. In terms of effectiveness, a decrease in load can be viewed as virtual energy storage discharge, while an increase in load can be perceived as virtual energy storage charging. The prevailing electricity price influences the electricity demand of users. When the electricity price is high, it indicates that users will reduce their load demand. Take 24 hours for the research period of demand side response, establish a user price-based demand response model, and the rules of user power consumption changes affected by real-time price changes in each period are as follows [26]:

$$\begin{bmatrix} \Delta P_1/P_1 \\ \Delta P_2/P_2 \\ \vdots \\ \Delta P_{24}/P_{24} \end{bmatrix} = [r_{i,j}]_{24\times 24} \begin{bmatrix} \Delta c_1/c_1 \\ \Delta c_2/c_2 \\ \vdots \\ \Delta c_{24}/c_{24} \end{bmatrix} \tag{12}$$

where ΔP indicates the amount of electricity consumption change in the i -th period; P_i indicates the power consumption of the i -th period; Δc_i indicates the amount of electricity price change in the i -th period; c_i indicates the price of electricity in the i -th period; r is a correlation matrix composed of self-elastic coefficients and mutual elastic coefficients.

Incentive demand-side response (IDR) involves the implementation of demand-side response contracts, enabling users to curtail specific loads during peak load periods, thereby achieving virtual energy storage and discharge effects. Price-based demand-side response encompasses various approaches such as interruptible load, demand-side bidding, emergency demand-side response, and direct load control [27]. Typically, the power department collaborates with load agencies to classify and aggregate users who can provide demand-side response resources, which are subsequently centrally regulated by the dispatch center. Different types of incentive demand-side response resources are categorized based on the speed of response to power grid dispatch instructions [28]. This paper primarily focuses on two types of incentive demand-side response resources. The first type involves load response within one hour, requiring user notification one day in advance and determining a calling plan during the day-ahead scheduling phase. The second type entails load response within 5-15 minutes, with users informed 15 minutes to 4 hours in advance. Due to the shorter response time, the calling plan is established during the daily scheduling phase. The amount of IDR load adjustment is limited by the response capacity and response speed, as follows:

$$\begin{cases} 0 \le \left|\Delta P_{IDR}^{t}\right| \le P_{IDR}^{\max} \\ \left|\Delta P_{IDR}^{t} - \Delta P_{IDR}^{t-1}\right| \le V_{IDR} \end{cases} \tag{13}$$

where $P_{IDR}^{\max}$ is the maximum response of the IDR load in the period t; V_{IDR} is the response rate of IDR load.

IV. DAY-AHEAD AND INTR-ADAY ECONOMIC DISPATCH MODEL

This paper proposes an economically optimal dispatch strategy from day-ahead and intra-day rolling dispatch scales. The framework for day-ahead and intra-day economic dispatch is illustrated in Fig. 3. The day-ahead scheduling operates hourly, accounting for multi-energy flexibility constraints and generating a 24-hour day-ahead operation plan for each equipment unit. The intra-day rolling scheduling aligns with the day-ahead strategy while considering the variations in the time scale adjustment between electric heating and gas energy. It is divided into long-term scale scheduling at the hourly level and short-term scale scheduling at the 15-minute class. Through continuous rolling optimization, the proposed strategy aims to minimize the impact of power fluctuations [29]. Given the discrepancies between day-ahead and intra-day forecasts of new energy and loads, the day-ahead scheduling considers the forecast volatility and the multi-energy flexibility of the system. This ensures that the day-ahead operation plan can effectively handle the differences between the day-ahead and intra-day forecasted power, providing the system with a flexible operational margin. Intra-day scheduling plays a crucial role in

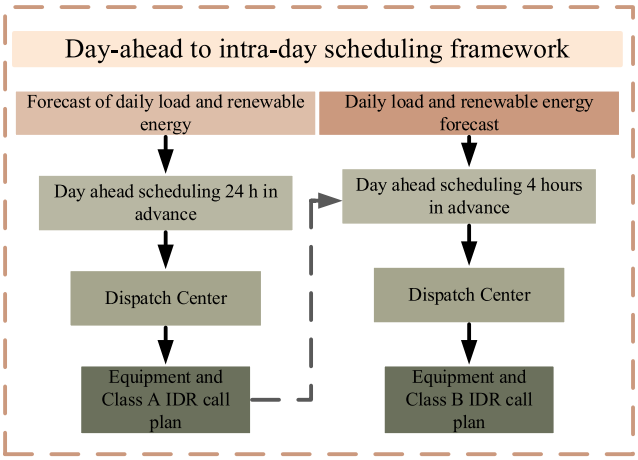

FIGURE 3. Day-ahead and intra-day scheduling framework.

stabilizing power fluctuations by adjusting the output of each device.

A. DAY-AHEAD SCHEDULING PHASE MODEL

The day-ahead scheduling plan is formulated 24 hours before, and the time scale is 1 hour. In the day-ahead stage, each unit output plan, price-based demand response load, and incentive-type demand response load call plan are required. They are substituted as a determined quantity into the intra-day dispatch stage [30]. The day-ahead scheduling is optimized to minimize the daily operating cost of the IES, and the objective function is:

$$\min \sum_{t=1}^{T} \left(F_u + F_{con} + F_{DA-IDR}\right) \tag{14}$$

where F_u indicates the cost of purchasing electricity and gas from the power grid and gas network; F_{con} indicates the maintenance and operation cost of each device; F_{DA-IDR} indicates the invocation cost of day-ahead incentive demand response.

$$F_u^t = \lambda_e^t P_{ebuy}^t + \lambda_g^t P_{gbuy}^t \tag{15}$$

$$\begin{aligned} F_{con}^t = {} & \lambda_{GT}^t \left(P_{GT}^t + Q_{GT}^t\right) + \lambda_{GB}^t P_{GB}^t + \lambda_{WH}^t P_{WH}^t + \lambda_{AC}^t P_{AC}^t \\ & + \lambda_{EL}^t P_{EL}^t + \lambda_{MR}^t P_{MR}^t + \lambda_{HFC}^t \left(P_{HFC}^t + Q_{HFC}^t\right) \\ & + \lambda_{GT}^t \left(Q_{HS-cha}^t + Q_{HS-dis}^t\right) \end{aligned} \tag{16}$$

$$F_{DA-IDR} = \sum_{t=1}^{T} K_{DA-IDR} \left|P_{DA-IDR}\right| \tag{17}$$

where λ_e^t and λ_g^t indicates the electricity price and gas price of the grid and gas network, respectively. λ_{GT}^t, λ_{GB}^t, λ_{WH}^t, λ_{AC}^t, λ_{EL}^t, λ_{HFC}^t indicates the maintenance price of GT, GB, WH, AC, EL, MR, HFC; K_{DA-IDR} represents the call coefficient of day ahead incentive demand response load; P_{DA-IDR} indicates the call volume of the day-ahead incentive demand response load period t .

The constraints of the day-ahead economic dispatch include the output constraints of each piece of equipment, the ramp rate constraints, the demand response resource constraints, and the capacity constraints of energy storage equipment. The constraints are shown in equations (18)∼(33):

$$P_{GT}^{\min} \le P_{GT}^t \le P_{GT}^{\max} \tag{18}$$
$$Q_{GT}^{\min} \le Q_{GT}^t \le Q_{GT}^{\max} \tag{19}$$
$$Q_{GB}^{\min} \le Q_{GB}^t \le Q_{GB}^{\max} \tag{20}$$
$$Q_{EB}^{\min} \le Q_{EB}^t \le Q_{EB}^{\max} \tag{21}$$
$$Q_{WH}^{\min} \le Q_{WH}^t \le Q_{WH}^{\max} \tag{22}$$
$$Q_{AR}^{\min} \le Q_{AR}^t \le Q_{AR}^{\max} \tag{23}$$
$$Q_{AC}^{\min} \le Q_{AC}^t \le Q_{AC}^{\max} \tag{24}$$
$$P_{EL}^{\min} \le P_{EL}^t \le P_{EL}^{\max} \tag{25}$$
$$P_{MR}^{\min} \le P_{MR}^t \le P_{MR}^{\max} \tag{26}$$
$$P_{HFC}^{\min} \le P_{HFC}^t \le P_{HFC}^{\max} \tag{27}$$
$$Q_{HS-cha}^{\min} \le Q_{HS-cha}^t \le Q_{HS-cha}^{\max} \tag{28}$$
$$\Delta P_{GT}^{\min} \le P_{GT}^{t+1} - P_{GT}^t \le \Delta P_{GT}^{\max} \tag{29}$$
$$\Delta P_{ELe}^{\min} \le P_{ELe}^{t+1} - P_{ELe}^t \le \Delta P_{ELe}^{\max} \tag{30}$$
$$\Delta P_{MRh}^{\min} \le P_{MRh}^{t+1} - P_{MRh}^t \le \Delta P_{MRh}^{\max} \tag{31}$$
$$\Delta P_{HFCh}^{\min} \le P_{HFCh}^{t+1} - P_{HFCh}^t \le \Delta P_{HFCh}^{\max} \tag{32}$$
$$S_{HS}^{\min} \le S_{HS} \le S_{HS}^{\max} \tag{33}$$

B. INTRA-DAY SCHEDULING PHASE MODEL

The intra-day scheduling plan is rolled every 15 minutes, and the scheduling plan after 4 hours of optimization is moved each time. The purpose is to correct the deviation between the previous scheduling plan and the intra-day working conditions [31]. In the intra-day stage, it is necessary to determine the output plan of each unit and the second type of incentive-type demand-side response load deployment plan. The daily scheduling stage takes the optimal system cost as the objective function, as shown in (34):

$$\min \sum_{t=1}^{T} \left(F_u + F_{con} + F_{IA-IDR}\right) \tag{34}$$

$$F_u^t = \lambda_e^t P_{ebuy}^t + \lambda_g^t P_{gbuy}^t \tag{35}$$

$$\begin{aligned} F_{con}^t = {} & \lambda_{GT}^t P_{GT}^t + \lambda_{GB}^t P_{GB}^t + \lambda_{WH}^t P_{WH}^t + \lambda_{AC}^t P_{AC}^t \\ & + \lambda_{EL}^t P_{EL}^t + \lambda_{MR}^t P_{MR}^t + \lambda_{HFC}^t P_{HFC}^t + \lambda_{GT}^t Q_{HS}^t \end{aligned} \tag{36}$$

$$F_{IA-IDR} = \sum_{t=1}^{T} K_{IA-IDR} \left|P_{IA-IDR}\right| \tag{37}$$

where F_{IA-IDR} indicates the invocation cost of intra-day incentive demand response; K_{IA-IDR} represents the call coefficient of intra-day incentive demand response load; P_{IA-IDR} indicates the call volume of the intra-day incentive demand response load period t .

TABLE 1. The process of optimizing scheduling.

Algorithm: A Rolling Optimization Scheduling Method for Day-ahead and Intra-day

Input: Predictive data for wind power, photovoltaic, and cooling, heating, and electrical loads (P_{PV}^{t} , P_{WT}^{t} , P_{eload}^{t} , P_{hload}^{t} , P_{cload}^{t} , T_{out})

Output: The optimal solution for system scheduling and the optimal economic cost of the system (F , $P_{\text{ebuy}}^{\text{t}}$, P_{gbuy}^{t} , P_{GT}^{t} , P_{HFC}^{t} , P_{EB}^{t} , P_{ELe}^{t} , Q_{EB}^{t} , Q_{EB}^{t} , Q_{AC}^{t} , Q_{HS-dis}^{t} , Q_{HS-cha}^{t} , Q_{HFC}^{t} , Q_{AR}^{t})

1: Set c_i

2: Set $P_i^{\max/\min}$, $Q_i^{\max/\min}$

***** Day-ahead economic dispatch *****

3: Set $t=1$

4: **for** $t \le 24$ **do**

5: Solve the problem (14)

6: **if** constraints (1)—(33) is feasible **then**

7: Derive an optimal solution, and obtain a system that can transfer electrical, cooling, and heating loads (P_{eload}^{tran} , P_{hload}^{tran} , P_{cload}^{tran})

8: Update $t=t+1$

9: **else**

10: Terminate

11: **end**

12: **end**

***** Intra-day economic dispatch *****

13: Set the (P_{eload}^{tran} , P_{hload}^{tran} , P_{cload}^{tran}) obtained in **Line 7** as input data and $t=1$

14: **for** $t \le 96$ **do**

15: Solve the problem (34)

16: **if** constraints (1)—(33) is feasible **then**

17: Derive an optimal solution

18: Update $t=t+1$

19: **else**

20: Terminate

21: **end**

22: **end**

The constraints of intra-day economic dispatching include the output constraints of each piece of equipment, the climbing rate constraints, the demand response resource constraints, and the capacity constraints of energy storage equipment. The constraints are the same as in (18)∼(33).

V. CASE STUDIES

A. CASE DESCRIPTION

A typical EH-IES is selected for case analysis, and the planning model established is a mixed integer programming model. Yalmip is an optimization solver integrating external optimization solvers (including Cplex) to form a unified modeling solution language. The optimization solution tool YALMIP is used to model and the CPLEX solver is used to solve the planning scheme. Table 1 describes the process of solving the optimal economic dispatch results for the system. The PV, WT, and load forecast curves are shown in Fig. 4. The parameters of energy conversion, supply, and storage devices are shown in Table 2. Energy prices are shown in Table 3. This paper analyzes four cases to verify the effectiveness of virtual energy storage in a day-ahead intra-day economic dispatch. The details of the cases are shown in Table 5.

To verify the significance of the proposed model in reducing carbon dioxide emissions, the wind PV and load data predicted in this paper are applied to the electric-hydrogen integrated energy system model presented in the form and the model proposed in the literature [32], respectively. We denote the model in the literature as EH-IES1, the model of the electric-hydrogen integrated energy system without virtual storage proposed in this paper as EH-IES2, and the electric-hydrogen integrated energy system without virtual storage is denoted as EH-IES3. The proposed model can

TABLE 2. Energy equipment parameters.

Parameter	Value	Parameter	Value (MW)
η_{GT}^{e}	0.7	$P_{GT}^{\max}$ $P_{GT}^{\min}$	300 0
η_{HFC}^{e}	0.95	$P_{HFC}^{\max}$ $P_{HFC}^{\min}$	300 0
η_{EL}	0.87	$P_{EL}^{\max}$ $P_{EL}^{\min}$	435 0
η_{EB}	0.9	$Q_{EB}^{\max}$ $Q_{EB}^{\min}$	300 0
η_{AC}	2.1	$Q_{AC}^{\max}$ $Q_{AC}^{\min}$	400 0
η_{GB}	0.9	$Q_{GB}^{\max}$ $Q_{GB}^{\min}$	300 0
η_{WH}	0.8	$Q_{WH}^{\max}$ $Q_{WH}^{\min}$	300 0
η_{AR}	1.2	$Q_{AR}^{\max}$ $Q_{AR}^{\min}$	300 0
η_{MR}	0.6	$P_{MR}^{\max}$ $P_{MR}^{\min}$	150 0
η_{HS}^{cha}	0.95	$Q_{HS-cha}^{\max}$ $Q_{HS-cha}^{\min}$	200 0
η_{HS}^{dis}	0.95	$Q_{HS-dis}^{\max}$ $Q_{HS-dis}^{\min}$	200 0

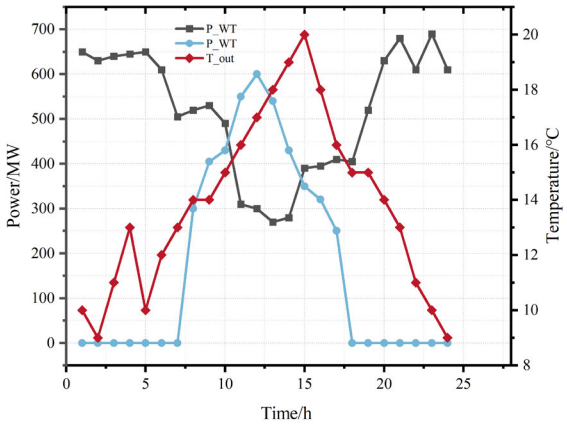

FIGURE 4. PV, WT, and load prediction.

TABLE 3. Energy purchase prices.

Period of time	Gas price (￥/MWh)	Electricity price (￥/MWh)
0:00~7:00	1.5	0.3438
8:00~11:00, 15:00~17:00		0.680
12:00~14:00, 18:00~22:00		0.811
23:00~24:00		0.380

TABLE 4. Comparison of different models of carbon trading.

	EH-IES1	EH-IES2	EH-IES3
Carbon emission (kg)	11700.70	99163.27	8000
Carbon transaction cost (￥)	4600.35	3331.63	2750

reduce the CO2 emission of the system by comparing the total carbon emission of the final design. Therefore, a carbon trading mechanism is added to the proposed model to facilitate obtaining CO2 emissions from the system. The carbon dioxide emissions and the system carbon trading cost between each model are shown in the table. Compared with the models proposed in the literature, the carbon emissions and carbon trading cost of EH-IES2 without virtual energy storage decreased by 24% and 31%, and the carbon emissions and carbon trading cost of EH-IES3 with virtual energy storage decreased by 32% and 41%. Therefore, the electric-hydrogen-integrated energy system model proposed in this paper can reduce CO2 emissions.

1) DAY-AHEAD ECONOMIC DISPATCH

The operating costs of each case in the day-ahead dispatch results are shown in Fig. 5. The system's total cost has the highest percentage of purchased energy, and the purchased energy cost of the system can be effectively reduced by including a virtual energy storage system. Case 1 has the highest price due to the absence of virtual energy storage. However, the addition of building virtual energy storage in Case 2 and demand side response virtual energy storage in

TABLE 5. Classification of case study.

Case	DR-VES	Building-VES
Case 1	×	×
Case 2	×	√
Case 3	√	×
Case 4	√	√

Case 3 reduces the cost by 1.25% and 4.62%, respectively, compared to Case 1. Adding both building and demand side response virtual energy Case 4 reduced the operating cost by 6.35% compared to Case 1. The results show that virtual energy storage effectively reduces the system cost and ensures the economic operation of the system.

This paper focuses on a detailed analysis of the operating characteristics of Case 4. The characteristic working curve of the day-ahead economic dispatch power system is presented in Fig. 6. In contrast, the operating angle of the day-ahead economic dispatch thermal system is shown in Fig. 7. Additionally, the operating curve of the day-ahead economic dispatch refrigeration system is shown in Fig. 8. These figures clearly illustrate that incorporating demand-side response and virtual energy storage enables adequate horizontal complementary substitution and vertical time shifting of loads. This can alleviate energy supply pressure, reduce the operating cost of the EH-IES, and unlock the optimization potential of the demand side. These benefits can be primarily attributed to two factors. Firstly, operators can selectively cut off or adjust the load power within the corresponding period as per the agreement, thereby mitigating energy supply pressure. Secondly, the load curve undergoes ''peak shaving and valley filling'' during peak hours, as some load power shifts to lower-demand periods.

Regarding electricity supply and demand, EH-IES prioritizes the purchase of electricity from the grid to supply users when electricity prices are low, and EH-ISE purchases less electricity from the grid when electricity prices are high. Due to the high wind at night, the excess electricity from the turbine is consumed by EL, EB, and AC, and the hydrogen produced by EL electrolysis ensures a stable supply of electricity from HFC to EH-IES. During the phase of high PV output, the excess electricity generated by PV can be consumed by EB and AC, which convert the electricity into heat and cold energy for supplying to the users. After adding demand-side response, users are guided to actively participate in demand response when the electricity price is low and the load increases. When the electricity price is high, the electric load demand of the user load decreases.

This paper maintains a fixed natural gas price for thermal supply and demand considerations. Within the EH-IES framework, natural gas procurement from the gas network is restricted to periods of elevated thermal load demand, which supplements GB and GT operations. Conversely, the thermal energy supply caters to the user's thermal load requirements during other time intervals. HFC and EB predominantly facilitate continuous heat energy provisioning throughout the day. Simultaneously, WH primarily alleviates potential heat

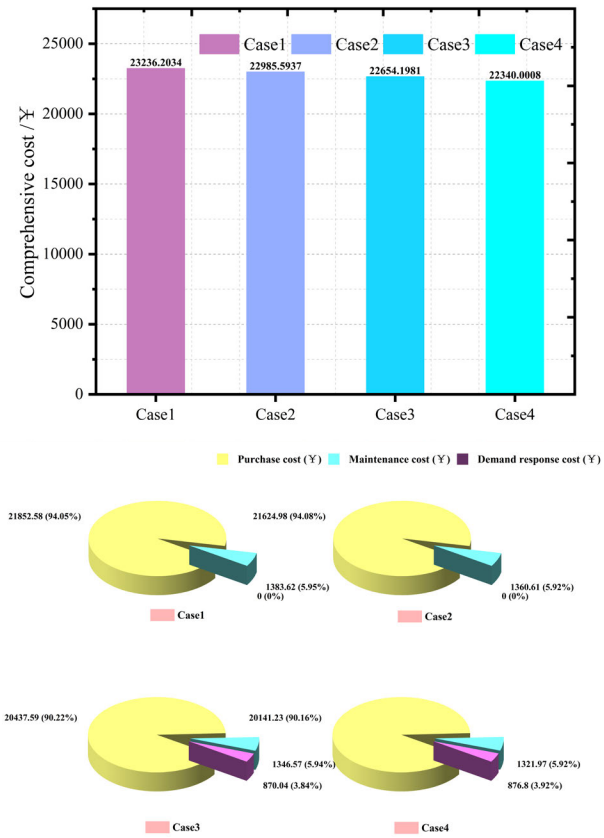

FIGURE 5. Total cost.

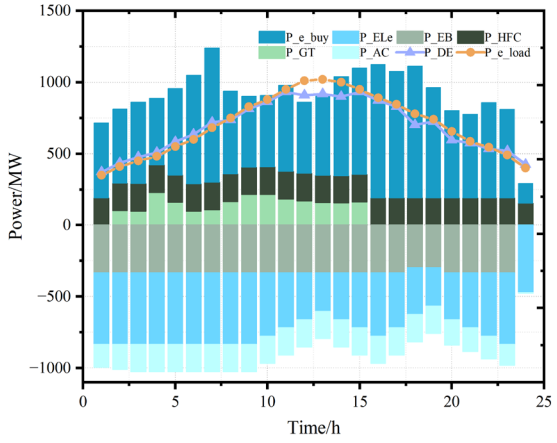

FIGURE 6. Day-ahead power system.

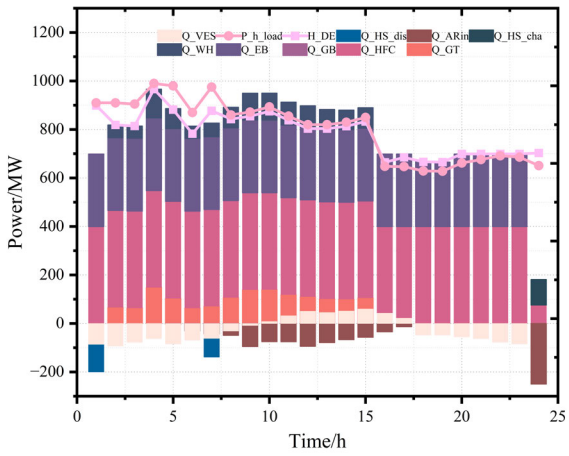

FIGURE 7. Day-ahead hot load.

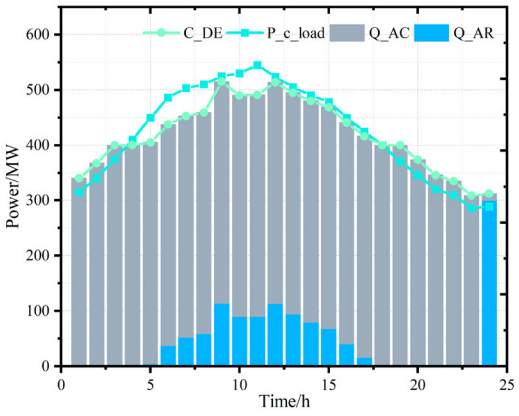

FIGURE 8. Day-ahead cold load.

energy shortages, while the HS system serves as a reservoir for storing and releasing heat energy when necessary. The integration of the building's VES makes distinct thermal phases evident. During the nighttime, the building's VES enters an exothermic stage influenced by outdoor temperature and lighting conditions. On the contrary, daytime operation transitions the building's VES into a heat storage phase due to heightened outdoor temperatures and daylight. Throughout these phases, the building's VES effectively manages the charging and discharging of heat energy, ensuring that indoor temperatures consistently remain within the user's predefined comfort range.

The supply and demand of cooling loads in the EH-IES system are addressed as follows. AC serves as the primary provider of cooling power to users, while AR functions to compensate for any potential shortage in cooling capacity. Excess heat generated by heating equipment can be absorbed by AR and transformed into the necessary cooling loads for users. Conversely, AC can convert excess electricity generated by power supply equipment, such as photovoltaic and wind power systems, into cooling energy that users can utilize.

B. INTRA-DAY ECONOMIC DISPATCH

The operating costs for each case are illustrated in Fig. 9. The daily wind power and photovoltaic prediction curves are presented in Fig. 10. The operating cost is the highest in Case 1, where no virtual energy storage system is implemented. Conversely, in Case 2 and Case 3, where building virtual energy storage and demand-side response virtual energy storage are integrated, the operating costs are reduced

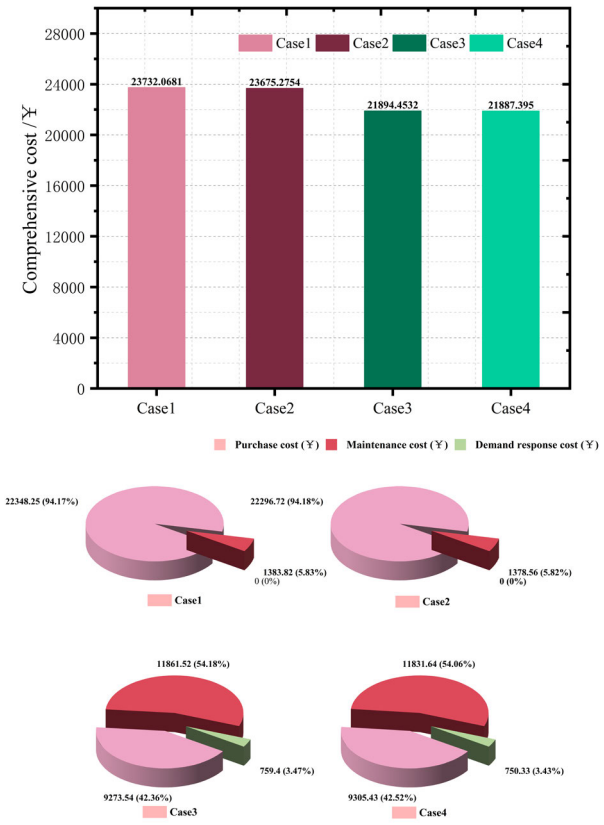

FIGURE 9. Total intra-day cost.

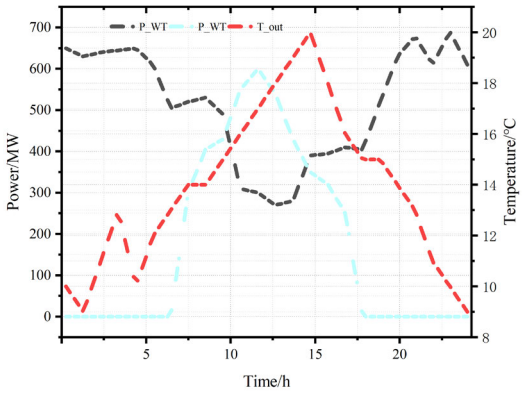

FIGURE 10. PV, WT, and load prediction.

by 0.24% and 7.74%, respectively, compared to Case 1. Furthermore, Case 4, which combines building and demand-side response virtual energy storage, exhibits a significant 13.04% reduction in operating costs compared to Case 1. These findings underscore the effectiveness of virtual energy storage in substantially reducing the system's operational expenses and ensuring its economic viability daily.

This paper focuses on a specific analysis of Case 4, where Figure 11 shows the operating characteristic curves of an intraday economically dispatched power system. In the

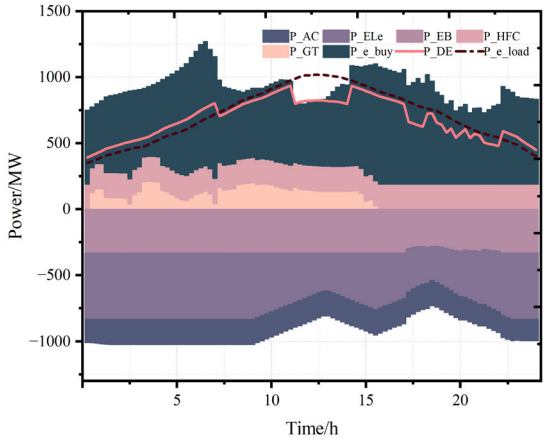

FIGURE 11. Intra-day electricity load.

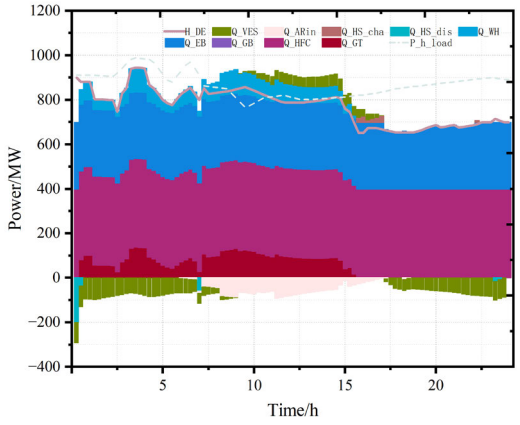

FIGURE 12. Intra-day hot load.

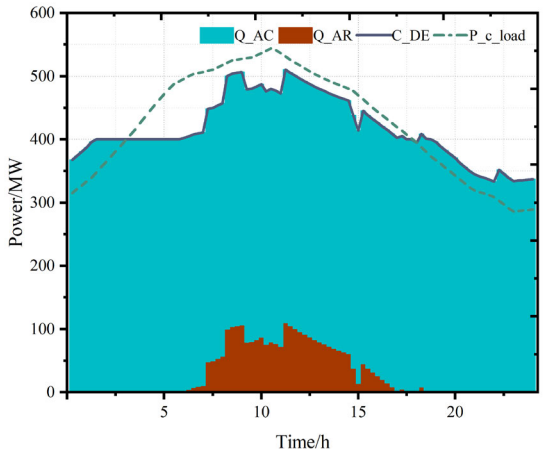

FIGURE 13. Intra-day cold load.

intraday dispatch phase, the system mainly purchases power from the grid, gas turbines, and hydrogen fuel cells are used as the primary energy supply equipment, and electric chillers, electric boilers, and electrolyzers translate the power into other forms of energy for the users. Figure 12 shows the operating characteristic curve of the thermal system for

intraday economic dispatch. In the intraday dispatch phase, the hydrogen fuel cell, waste heat boiler, and gas turbine are mainly responsible for the thermal energy supply of the system; the virtual energy storage system of the building plays a significant role in thermal storage, the heat storage tank is only helpful at night, and the absorption chiller is the primary heat utilization device, which converts heat energy into cold energy to supply to the users. Figure 13 shows the operating characteristic curve of the cooling system for the intraday economic dispatch. Adding demand-side response VSE in the intraday phase can improve the load's operating angle and reduce the EH-IES operating cost. The intraday stage mainly invokes the incentive-based demand-side response, in which the users especially switch the switchable gears off through circuit breakers.

The results of Case 4 in the day-ahead scheduling are used as the basis for the day-ahead plan. In this paper, considering the fluctuation of predicted wind power and photovoltaic temperature, long-term optimization in the day is carried out to stabilize power fluctuations by adjusting the equipment output following the output status of each gear identified in the day-ahead scheduling in Case 4.

VI. CONCLUSION

An electric hydrogen comprehensive energy system that incorporates virtual energy storage was constructed in this paper. A multi-time scale scheduling strategy was proposed, which included day-ahead and intra-day scheduling, to suppress the fluctuation of electric heating and cooling power. The minimum cost under optimal economic scheduling was obtained by constructing objective functions for day-ahead and intra-day scheduling and setting constraints on given conditions. The changes in operating expenses of the system were evaluated through comparative studies on four cases. Finally, case simulations were conducted based on predicted PV, WT, load, and indoor temperature data using the YALMIP toolbox and the CPLEX solver. However, hydrogen storage can help balance the mismatch between energy supply and demand, especially for unstable renewable energy. It can store excess energy and release it when needed. In the existing models, we have yet to consider hydrogen energy storage and the impact of seasonal characteristics on renewable energy and energy storage.

In future work, we plan to tackle the issues above by employing advanced multi-objective intelligent algorithms. Specifically, our focus will be on considering the influence of seasonal energy storage on the system and the impact of system capacity configuration on system scheduling.

REFERENCES

[1] Y. Wang, Y. Wang, Y. Huang, H. Yu, R. Du, F. Zhang, F. Zhang, and J. Zhu, "Optimal scheduling of the regional integrated energy system considering economy and environment," *IEEE Trans. Sustain. Energy*, vol. 10, no. 4, pp. 1939–1949, Oct. 2019.

[2] H. Li, N. Zhang, C. Kang, G. Xie, and Q. Li, "Analytics of ontribution degree for renewable energy accommodation factors," *Proc. CSEE*, vol. 39, no. 4, pp. 1009–1017, Feb. 2019.

[3] Z. Zhang, C. Wang, H. Lv, F. Liu, H. Sheng, and M. Yang, "Day-ahead optimal dispatch for integrated energy system considering power-to-gas and dynamic pipeline networks," *IEEE Trans. Ind. Appl.*, vol. 57, no. 4, pp. 3317–3328, Jul. 2021.

[4] R. Zhang, T. Jiang, F. Li, G. Li, H. Chen, and X. Li, "Coordinated bidding strategy of wind farms and power-to-gas facilities using a cooperative game approach," *IEEE Trans. Sustain. Energy*, vol. 11, no. 4, pp. 2545–2555, Oct. 2020.

[5] Y. Iwafune, O. Kazuhiko, Y. Kobayashi, K. Suzuki, and Y. Shimoda, "Aggregation model of various demand-side energy resources in the day-ahead electricity market and imbalance pricing system," *Int. J. Electr. Power Energy Syst.*, vol. 147, May 2023, Art. no. 108875.

[6] X. Wang, Z. Bie, F. Liu, Y. Kou, and L. Jiang, "Bi-level planning for integrated electricity and natural gas systems with wind power and natural gas storage," *Int. J. Electr. Power Energy Syst.*, vol. 118, Jun. 2020, Art. no. 105738.

[7] Y. Zheng, J. Wang, S. You, X. Li, H. W. Bindner, and M. Münster, "Data-driven scheme for optimal day-ahead operation of a wind/hydrogen system under multiple uncertainties," *Appl. Energy*, vol. 329, Jan. 2023, Art. no. 120201.

[8] M. Li, L. Huang, and Y. Li, "Optimal dispatch of integrated electricity-gas-heat system considering power to gas," in *Proc. 33rd Chin. Control Decis. Conf. (CCDC)*, May 2021, pp. 944–949.

[9] B. Koirala, S. Hers, G. Morales-España, Ö. Özdemir, J. Sijm, and M. Weeda, "Integrated electricity, hydrogen and methane system modelling framework: Application to the Dutch infrastructure outlook 2050," *Appl. Energy*, vol. 289, May 2021, Art. no. 116713.

[10] Q. Wang, Y. Wang, and Z. Chen, "Day-ahead economic optimization scheduling model for electricity–hydrogen collaboration market," *Energy Rep.*, vol. 8, pp. 1320–1327, Nov. 2022.

[11] X. Liu, "Multiple time-scale economic dispatching strategy for commercial building with virtual energy storage under demand response mechanism," *Int. J. Energy Res.*, vol. 45, no. 11, pp. 16204–16227, Sep. 2021.

[12] G. Lv, Y. Ji, Y. Zhang, W. Wang, J. Zhang, J. Chen, and Y. Nie, "Optimization of building microgrid energy system based on virtual energy storage," *Frontiers Energy Res.*, vol. 10, p. 1910, Jan. 2023.

[13] N. S. Raman and P. Barooah, "On the round-trip efficiency of an HVAC-based virtual battery," *IEEE Trans. Smart Grid*, vol. 11, no. 1, pp. 403–410, Jan. 2020.

[14] P. Li, Z. Wang, N. Wang, W. Yang, M. Li, X. Zhou, Y. Yin, J. Wang, and T. Guo, "Stochastic robust optimal operation of community integrated energy system based on integrated demand response," *Int. J. Electr. Power Energy Syst.*, vol. 128, Jun. 2021, Art. no. 106735.

[15] Y. Li, M. Han, Z. Yang, and G. Li, "Coordinating flexible demand response and renewable uncertainties for scheduling of community integrated energy systems with an electric vehicle charging station: A bi-level approach," *IEEE Trans. Sustain. Energy*, vol. 12, no. 4, pp. 2321–2331, Oct. 2021.

[16] L. Zhang, W. Dai, B. Zhao, X. Zhang, M. Liu, Q. Wu, and J. Chen, "Multi-time-scale economic scheduling method for electro-hydrogen integrated energy system based on day-ahead long-time-scale and intra-day MPC hierarchical rolling optimization," *Frontiers Energy Res.*, vol. 11, Feb. 2023, Art. no. 1132005.

[17] S. Cheng, R. Wang, J. Xu, and Z. Wei, "Multi-time scale coordinated optimization of an energy hub in the integrated energy system with multi-type energy storage systems," *Sustain. Energy Technol. Assessments*, vol. 47, Oct. 2021, Art. no. 101327.

[18] X. Li, W. Wang, and H. Wang, "Hybrid time-scale energy optimal scheduling strategy for integrated energy system with bilateral interaction with supply and demand," *Appl. Energy*, vol. 285, Mar. 2021, Art. no. 116458.

[19] X. Huang, K. Wang, M. Zhao, J. Huan, Y. Yu, K. Jiang, X. Yan, and N. Liu, "Optimal dispatch and control strategy of integrated energy system considering multiple P2H to provide integrated demand response," *Frontiers Energy Res.*, vol. 9, p. 925, Jan. 2022.

[20] Y. Bo, Y. Xia, and W. Wei, "Ultra-short-term optimal dispatch for EH-IES considering uncertainty of delay in the distribution network," *Int. J. Electr. Power Energy Syst.*, vol. 141, Oct. 2022, Art. no. 108214.

[21] M. Kazemi, S. Y. Salehpour, F. Shahbaazy, S. Behzadpoor, S. Pirouzi, and S. Jafarpour, "Participation of energy storage-based flexible hubs in day-ahead reserve regulation and energy markets based on a coordinated energy management strategy," *Int. Trans. Electr. Energy Syst.*, vol. 2022, pp. 1–17, Sep. 2022.

[22] Y. Gong, X. Yang, J. Xu, C. Chen, T. Zhao, S. Liu, Z. Lin, L. Yang, H. Qian, and C. Ke, "Optimal operation of integrated energy system considering virtual heating energy storage," *Energy Rep.*, vol. 7, pp. 419–425, Apr. 2021.
[23] Y. Shen, X. Liang, W. Hu, X. Dou, and F. Yang, "Optimal dispatch of regional integrated energy system based on a generalized energy storage model," *IEEE Access*, vol. 9, pp. 1546–1555, 2021.
[24] D. Zhang, H. Zhu, H. Zhang, H. H. Goh, H. Liu, and T. Wu, "Multi-objective optimization for smart integrated energy system considering demand responses and dynamic prices," *IEEE Trans. Smart Grid*, vol. 13, no. 2, pp. 1100–1112, Mar. 2022.
[25] T. Song, Y. Li, X.-P. Zhang, C. Wu, J. Li, Y. Guo, and H. Gu, "Integrated port energy system considering integrated demand response and energy interconnection," *Int. J. Electr. Power Energy Syst.*, vol. 117, May 2020, Art. no. 105654.
[26] H. Ebrahimi, A. Yazdaninejadi, and S. Golshannavaz, "Decentralized prioritization of demand response programs in multi-area power grids based on the security considerations," *ISA Trans.*, vol. 134, pp. 396–408, Mar. 2023.
[27] H. Yang, M. Li, Z. Jiang, and P. Zhang, "Multi-time scale optimal scheduling of regional integrated energy systems considering integrated demand response," *IEEE Access*, vol. 8, pp. 5080–5090, 2020.
[28] Z. Yang, M. Ni, and H. Liu, "Pricing strategy of multi-energy provider considering integrated demand response," *IEEE Access*, vol. 8, pp. 149041–149051, 2020.
[29] X. Yang, Z. Chen, X. Huang, R. Li, S. Xu, and C. Yang, "Robust capacity optimization methods for integrated energy systems considering demand response and thermal comfort," *Energy*, vol. 221, Apr. 2021, Art. no. 119727.
[30] L. Tian, C. Zhu, and T. Deng, "Day-ahead scheduling of SMR integrated energy system considering heat-electric-cold demand coupling response characteristics," *Energy Rep.*, vol. 8, pp. 13302–13319, Nov. 2022.
[31] L. Chen, H. Tang, J. Wu, C. Li, and Y. Wang, "A robust optimization framework for energy management of CCHP users with integrated demand response in electricity market," *Int. J. Electr. Power Energy Syst.*, vol. 141, Oct. 2022, Art. no. 108181.
[32] J. Chen, Z. J. Hu, and Y. G. Chen, "Thermoelectric optimization of integrated energy system considering ladder-type carbon trading mechanism and electric hydrogen production," *Electr. Power Autom. Equip.*, vol. 41, pp. 48–55, Jun. 2021.

XINGHUA LIU (Senior Member, IEEE) received the B.Sc. degree from Jilin University, Changchun, China, in 2009, and the Ph.D. degree in automation from the University of Science and Technology of China, Hefei, China, in 2014.

From 2014 to 2015, he was a Visiting Fellow with RMIT University, Melbourne, VIC, Australia. From 2015 to 2018, he was a Research Fellow with the School of Electrical and Electronic Engineering, Nanyang Technological University, Singapore. He has been a Professor with the Xi'an University of Technology, Xi'an, China, since 2018. His current research interests include integrated energy systems, intelligent systems, cyber-physical systems, robotic systems, state estimation and control, and autonomous vehicles.

LONGYU ZU (Student Member, IEEE) received the B.S. degree in electrical engineering from Qufu Normal University, Rizhao, in July 2022. She is currently pursuing the M.S. degree with the Xi'an University of Technology, Xi'an, China. Her current research interest includes the economic dispatch of integrated energy systems.

XIANG LI (Student Member, IEEE) received the B.S. degree in electrical engineering from the Xi'an University of Technology, Xi'an, China, in July 2020, where he is currently pursuing the M.S. degree. His current research interests include the economic dispatch of integrated energy systems and low-carbon technology.

HUIBAO WU received the degree in power generation and power system automation from the Xi'an Electric Power College. He has been with State Grid Xi'an Power Supply Company, since 1998. His current research interest includes power system operation and management.

RONG HA received the B.S. degree in computer information management from Xidian University. He has been with Xi'an Jinze Electric Technology Company Ltd., since 2014. His current research interests include system integration and reliability design.

PENG WANG (Fellow, IEEE) received the B.Sc. degree in electrical engineering from Xi'an Jiaotong University, Xi'an, China, in 1978, the M.Sc. degree from the Taiyuan University of Technology, Taiyuan, China, in 1987, and the M.Sc. and Ph.D. degrees in electrical engineering from the University of Saskatchewan, Saskatoon, SK, Canada, in 1995 and 1998, respectively.

He is currently a Professor with Nanyang Technological University, Singapore. His current research interests include power system planning and operation, renewable energy planning, solar/electricity conversion systems, and power system reliability analysis. He served as an Associate Editor of IEEE TRANSACTION ON SMART GRIDS and a Guest Editor for the Special Issues on Smart Grids of *Journal of Modern Power Systems and Clean Energy*. He also served as an Associate Editor for IEEE TRANSACTION ON POWER DELIVERY and the Guest Editor-in-Chief for the Special Issues on Hybrid AC/DC Grids for Future Power Systems of *CSEE Journal of Power and Energy Systems*.